

An integrator based wind speed estimator for wind turbine control

Younes Ait Elmaati^{*}, Lhoussain El Bahir^a and Khalid Faitah^b

Laboratory of Electrical Engineering and Control Systems (LGE COS), National School of Applied Sciences, Cadi Ayyad University, Av. Abdelkarim El khattabi B.P 575, Marrakech 40000, Morocco

(Received June 28, 2015, Revised October 10, 2015, Accepted October 13, 2015)

Abstract. In this paper, an integrator based method to estimate the effective wind speed in wind turbine systems is proposed. First, the aerodynamic torque was accurately estimated through a proportional gain based observer where the generator speed is the measured output of the system. The torque signal contains not only useful frequencies of the wind, but also high frequencies and the ones due to structural vibration. The useful information of the wind signal is low frequency. A spectral analysis permitted the determination of the useful frequencies. The high frequencies were then filtered before introducing the torque signal in the wind speed observer. The desired effective wind speed was extracted through an integrator based observer using the previously estimated aerodynamic torque. The strength of the method is to avoid numerical solutions used in literature of the wind speed estimation. The effectiveness of the proposed wind speed estimator and its use to control the generator speed has been tested under turbulent situations using the FAST software (Fatigue, Aerodynamics, Structures, and Turbulence), for large scale Megawatt turbine.

Keywords: feed forward control; wind turbine power generation system; wind speed estimation; wind turbine control; FAST software

1. Introduction

A wind turbine is a device for extracting energy from the wind. Fig. 1 shows the basic components, including blades, hub, low and high speed shaft, gearbox, generator, nacelle and tower.

The increasing energy demand leads to the production of large wind turbines. Thus, more and more vibrational behaviors could be expected. A wind turbine may exhibit various motions due to several factors, such as rotor and generator rotation, nacelle yaw degree of freedom and elastic deflections of blade and the tower.

In terms of control, Wright and Balas (2003), Laks *et al.* (2009), Boukhezzar *et al.* (2007), Novak *et al.* (1995), the wind turbine operates in two distinct regions. At low wind speeds, in the partial load region, the turbine is controlled to maximize the power output as studied in Kodama *et al.* (2000). The power maximization is achieved by adjusting the generator torque to keep an

*Corresponding author, Ph.D. Student, E-mail: aitelmaati.younes@gmail.com

^a Ph.D., E-mail: l.elbahir@uca.ma

^b Ph.D., E-mail: k.faitah@uca.ma

optimum ratio between the tip speed of the blades and the wind speed. At higher wind speeds, in the full load region, the wind turbine is controlled to reduce loads by producing a rated power output at a constant rotor speed, Ohtsubo and Kajiwara (2004). This is obtained by pitching the blades to adjust the efficiency of the rotor, while applying a constant generator torque as in Wright *et al.* (2007), Pao and Johnoson (2009). The estimation of the wind speed could be used in fault tolerant control, Sloth *et al.* (2011). Wind speed could also be used to design a linear parameter varying controller for the speed control as in Hammerum *et al.* (2007) and Jabbari (1997).

The wind speed has a huge impact on the dynamic response of wind turbine. Many control algorithms use a measure of the wind speed to increase performance of the turbine. Unfortunately, no accurate measurement of the effective wind speed is available from a direct measurement. In most turbines, wind speed is measured by anemometers, which are potentially exposed to faults as studied in Beltrán *et al.* (2012) and vibrations noises. Then, the wind speed estimator could be an analytical redundancy of the faulty sensor.

Several methods have been proposed in literature for wind speed estimation. Methods based on fitting wind data according to a distribution are proposed in Garcia *et al.* and (1998), Hui *et al.* (2014) and Sedghi *et al.* (2015). Justus *et al.* (1978) proposed a method for estimating wind speed frequency distributions. Statistical methods used to estimate extreme wind speeds are presented and discussed Perrin *et al.* (2006). In Mohandes *et al.* (2011), a method is proposed for generating wind speed profile based on knowledge of wind speed at lower heights using adaptive neuro-fuzzy inference system. Authors in Kusiak and Li (2010) presented a method for prediction of wind speed at a selected location based on the data collected at neighborhood locations. Several parameters could influence wind speed estimation (spatiotemporal data resolution, micrometeorological characterization, and extreme value statistics), a study was conducted by Lombardo (2012) to investigate factors that can influence extreme wind estimation.

Another set of wind estimation approaches use measurements from the structure itself. In our work the structure is a large scale wind turbine. Many previous works have dealt with this issue. In Bourlis and Bleijs (2010), the estimation algorithm consists of an adapting Kalman filter, estimating the aerodynamic torque acting on the rotor of the turbine, then a Newton-Raphson method, derives the effective wind speed from the aerodynamic torque.

The last method has the drawback to have more than a unique solution for small pitch angles as stated in Østergaard *et al.* (2007). Other wind speed estimation algorithms, based on optimization approach, can be found in Hafidi and Chauvin, (2012), Bhowmik and Rene (1998) and Chauvin and Petit (2010). Methods relying on learning machines are studied in Wu *et al.* (2013).

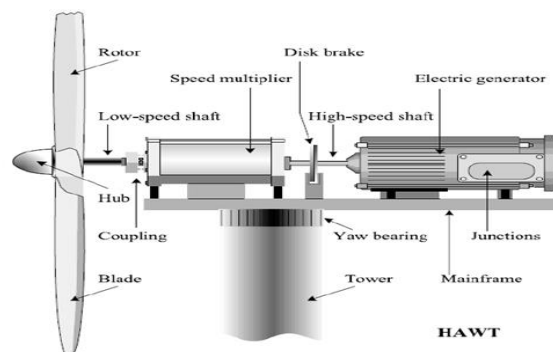


Fig. 1 Wind turbine constitution

The online estimated wind speed could be used in feed forward control of wind turbines as in van der Hooft and van Engelen (2004). Authors in Bhowmik and Rene (1998) have used wind speed estimation for power generation improvement through maximum power point tracking. One can find further details on improving power curve modelling using wind speed in Cutler *et al.* (2012). The estimation could also be used for wind turbine extreme gust control as in Kanev and van Engelen (2010). Wind turbine control capabilities could furthermore be improved when using combination of wind estimation and short term prediction of wind speed as studied in Spencer *et al.* (2013). Deepa and Sheela (2014) presented a method to fix hidden neuron in multilayer perceptron networks for wind speed prediction. Seguro and Lambert (2000) have proposed an alternative for estimation of the parameters of the weibull wind speed distribution dedicated for wind energy analysis. For more details, a comparison of these methods could be found in An and Pandley (2005).

The majority of the previously mentioned methods, when applied on the wind turbine structure, begin by estimating the aerodynamic torque because it is the only measurement that contains direct information about the wind shape and amplitude. Most of the turbine measurement based approaches uses the Newton Raphson numerical resolution to extract the wind speed. However, this method has not a unique solution for wind speed near the small pitch angles since the function to solve is non injective.

In this paper, an integrator based method to estimate the effective wind speed in wind turbine systems is proposed. As a first step, the aerodynamic torque is estimated through a proportional based observer loop designed for an augmented model of the turbine mechanical part; where the measured generator speed is considered as a reference signal and the control signal applied on the model represents implicitly the estimated torque. In the second step, an integrator based observer is used to perform the estimation of the wind speed using the previously estimated aerodynamic torque as reference signal. The contribution of this technique is to use the integrator based estimator in extracting the wind speed. This technique avoids numerical resolution studied in the previously mentioned works. The method is implemented in FAST software, developed by the National Renewable Energy Laboratory (NREL), for large scale Megawatt turbine.

This paper is organized as follows. In section 2, the wind turbine model is presented and discussed. In section 3, the estimation method of the aerodynamic torque is studied. Then, section 4 will deal with reconstruction of the wind speed using the previously estimated aerodynamic torque. The effectiveness of the wind speed estimation is studied in section 5 through wind turbine control over the operation range. Finally, the section 6 will present the conclusion of the paper and give some perspectives.

2. Turbine model

From a mechanical point of view, the wind turbine can be approximated by two rigid bodies interconnected by an equivalent shaft in which all parameters of the generator (inertia, torque, speed...) are cast to the equivalent low speed shaft as in Fig. 2. The equivalent shaft is modelled by a flexible body with a damping and stiffness as in Bongers (1994).

2.1 Aerodynamic model

A pure aerodynamic torque is applied to the rotor by the wind and is given by

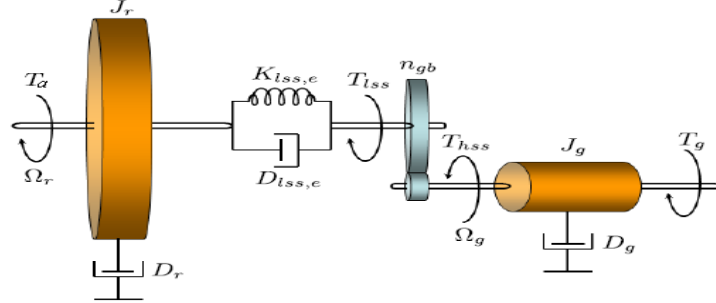


Fig. 2 Two bodies approximation of drive train

$$T_a = \frac{1}{2} \rho \pi R^3 V^2 C_q(V, \Omega_r, \beta) \quad (1)$$

Where $C_q(V, \Omega_r, \beta) = \frac{1}{\lambda} C_p(V, \Omega_r, \beta)$ and $\lambda = \frac{1}{V} R \Omega_r$.

ρ is the air density, R is the radius of the rotor, V is the wind speed, Ω_r is the rotor speed, β is the pitch angle, C_q and C_p are the torque and power coefficients respectively and are turbine dependent. λ is the tip speed ratio. It is used to maintain the wind turbine at a desired performance by fixing λ at a suitable value. C_p is provided by the constructor and can be simulated as a look up table. In most cases, only few points of C_p are given with the datasheet of the turbine (see Khalil (2007)). Since no exact expression of C_p is known, the following approximation is often used:

$$C_p(\lambda, \beta) = C_1(C_2M - C_3\beta - C_4)^{C_5N} + C_6\lambda, \text{ where } N = \frac{0.0035}{(1+\beta^3)(\lambda+0.08\beta)} \text{ and } M = \frac{1}{(\lambda+0.08\beta)} - \frac{0.035}{(1+\beta^3)}$$

With $C_1 = 0.5176$; $C_2 = 116$; $C_3 = 0.4$; $C_4 = 5$; $C_5 = 21$; $C_6 = 0.0068$.

This torque is transmitted to the generator through the drive train approximated with one low speed shaft having a damping and stiffness. In Jonkman and Buhl (2005), the generator receives a low speed shaft torque given by

$$T_{lss,e} = D_{lss,e}(\Omega_r - \Omega_g) + K_{lss,e}(\theta_r - \theta_g) \quad (2)$$

θ_r and θ_g are the equivalent shaft rotational angles of the rotor side and the generator side respectively. Ω_r is the rotor speed and Ω_g is the generator speed. $K_{lss,e}$ and $D_{lss,e}$ are the stiffness and the damping of the drive train. Notice that the generator speed, angle and inertia considered in this paper are about the equivalent low speed shaft and not about the high speed shaft.

2.2 Drive train model

The drive train is composed of a low speed shaft (rotor side) interconnected with a high-speed shaft (generator side) through a mechanical gearbox with a ratio N_g . The drive train is modelled by the following differential equations

$$\dot{\Omega}_r = \frac{D_{lss,e}}{J_r} \Omega_r - \frac{X}{J_r} + \frac{D_{lss,e}}{J_r} \Omega_g + \frac{T_a}{J_r} \quad (3)$$

$$\dot{X} = K_{lss,e}\Omega_r - K_{lss,e}\Omega_g \quad (4)$$

$$\dot{\Omega}_g = \frac{D_{lss,e}}{J_g}\Omega_r - \frac{X}{J_g} + \frac{D_{lss,e}}{J_g}\Omega_g + \frac{N_g T_g}{J_g} \quad (5)$$

J_r is the Rotor inertia, J_g is the generator inertia, X is the restoring force applied on the low speed shaft. The shaft is driven by the aerodynamic torque. The generator torque about the equivalent low speed shaft $N_g T_g$ is used to accelerate or decelerate the shaft.

2.3 The wind model

The wind profile used in this simulation follows the Kaimal distribution, with 9 m/s of mean and 30% of turbulence according to the International Electrotechnical Commission standards (IEC). Fig. 3 shows the wind profile considered in simulation.

Table 1 Turbine characteristics

Characteristic	Value
Rated power (MW)	1.5
Rotor diameter (m)	70
Blade mass (Kg)	4,230
Hub mass (Kg)	15,104
Total rotor mass (Kg)	32,016
$K_{lss,e}$: Stiffness of equivalent shaft (N·m/rad)	$5.6 \cdot 10^9$
$D_{lss,e}$: Damping of equivalent shaft (N·m/rad/s)	$1 \cdot 10^7$
J_r : Rotor Inertia (kg·m ²)	$2.9624 \cdot 10^6$
N_g : Gearbox Ratio	87.965
J_g : Generator Inertia (kg·m ²)	$53.036 \cdot N_g^2$
R : Rotor radius (m)	35
V_N : Rated wind speed (m/s)	12
$V_{\Omega N}$: Nominal wind speed (m/s)	10
Ω_N : Turbine rotor rated speed (rad/s)	2
Ω_{VN} : Rotor speed at rated power (rad/s)	1.6
ρ : air density (kg/m ³)	1.225

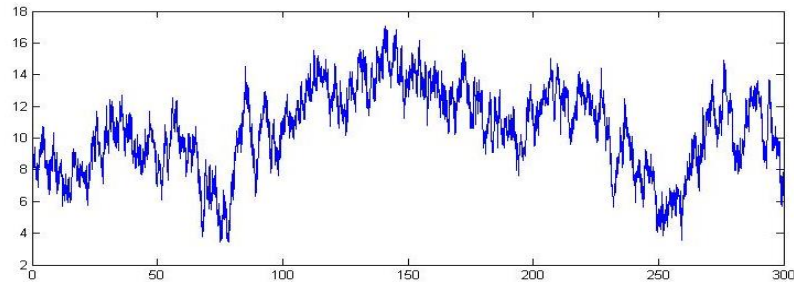


Fig. 3 Used turbulent wind speed (m/s)

2.4 The FAST software (*Fatigue, Aerodynamics, Structures, and Turbulence*)

The FAST (Fatigue, Aerodynamics, Structures, and Turbulence) code (Jonkman and Buhl (2005) and the references therein) is an aeroelastic simulator capable of predicting both the extreme and fatigue loads of two- and three-bladed flexible horizontal-axis wind turbines (HAWTs) with 24 degrees of freedom. The code uses a modal approach in combination with Kane Dynamics to develop the equations of motion. FAST helps considerably researchers and engineers in testing wind loads reduction algorithms (Jong-Won *et al.* 2013). Another relevant field of research is testing the effect of faults and fault tolerant control strategies on the different loads of the turbine. The last test leads to decide on the suitable algorithm to use in order to avoid excitation of the turbine vibrational modes.

In this research, FAST has been used to model an upwind, three-bladed rotor HAWT with a rigid foundation, considering 23 of 24 degrees of freedom including first and second flapwise blade mode, edgewise blade mode, drivetrain rotational flexibility, first and second tower fore-aft bending mode, first and second tower side-to-side bending mode and generator azimuth angle.

FAST reads mechanical system parameters from input files (the blade airfoil characteristics file, the tower structure file ...), and creates output files (providing measurement of the wind turbine outputs such as torques, speeds, deflections, moments on blades and tower ...). Moreover, it can be used to exchange data with Simulink (the Simulink software provides the pitch angle, the torque and the yaw angle as inputs to the FAST model). The controllers and the electrical parts of a wind turbine can be implemented by personalized Simulink blocks where the mechanical parts of a wind turbine are simulated by FAST.

The used wind profile is generated by the Turbsim simulator (Jonkman and Buhl (2007) as an input file to FAST. TurbSim is a stochastic, full-field, turbulent-wind simulator used to provide simulated inflow turbulence environments that incorporate many of the important fluid dynamic features known to affect turbine modes and loading, such as tower shadow and wind shear.

3. Aerodynamic torque estimation

3.1 Torque estimation loop

In literature, many approaches have been proposed for aerodynamic torque estimation. Østergaard *et al.* (2007) proposed a PI based observer to estimate aerodynamic torque. In Hafidi

and Chauvin (2012), authors used the Kalman filter to reconstruct the aerodynamic torque Fourier coefficients.

In this paper, the proposed method is based on the transfer function between the aerodynamic torque T_a and the rotor speed Ω_r . However in most cases, the rotor speed cannot be measured; the measured generator speed about low speed shaft could be considered as a good approximation to the rotor speed. In fact, after transients, the rotor and generator speed about the equivalent low speed shaft are the same, in the case of a rigid equivalent shaft, or when damping the torsional modes of the mechanical shaft.

The transfer function $F(s)$, between the aerodynamic torque T_a and generator speed Ω_r is obtained after manipulations of Eqs. (3)-(5) as follow:

$$F(s) = \frac{1}{s} \frac{as+b}{(s^2+cs+d)}, \text{ where } a = \frac{D_{lss,e}}{J_r J_g}; b = \frac{K_{lss,e}}{J_r J_g}; c = \left(\frac{J_r+J_g}{J_r J_g}\right) D_{lss,e}; d = K_{lss,e} \left(\frac{J_r+J_g}{J_r J_g}\right)$$

The idea is to keep the model speed Ω_{gm} sufficiently close to the measured one, Ω_g , by acting on the model with an adequate aerodynamic torque \hat{T}_a . This could be performed through a feedback estimation loop as presented in Fig. 4. In contrast to authors in the previous works, and since the transfer function $F(s)$ already contains an integrator term, and assumed that the mean of Ω_g is sufficiently low frequency, only a proportional action is needed to estimate T_a . After transients, the model output Ω_{gm} converges to Ω_g and its input \hat{T}_a converges to the actual torque T_a . Finally, \hat{T}_a can be considered as an estimation of the actual aerodynamic torque T_a . The proportional torque estimator gain, is chosen in such way that the slowest pole of the closed loop of the transfer function $F(s)$ is cancelled. The method for estimating the torque is tested under turbulent wind and all turbine degrees of freedom are activated in the FAST software. Fig. 5 shows the actual and estimated aerodynamic torque. The actual aerodynamic torque represented in Fig. 5 by the red color is obtained by the following equation:

$$T_a = \text{Rotor}_{\text{Acceleration}} * J_r * \frac{\pi}{180} + \text{Shaft}_{\text{Torque}} * 1000$$

J_r is the rotor inertia about the shaft of the turbine. The shaft torque (KNm) and the rotor acceleration (deg/sec²) can be obtained from FAST software as outputs. In the industrial wind turbines, a strain gauge is installed on the mechanical shaft of the wind turbine to measure the shaft torque. The rotor acceleration is measured by an accelerometer.

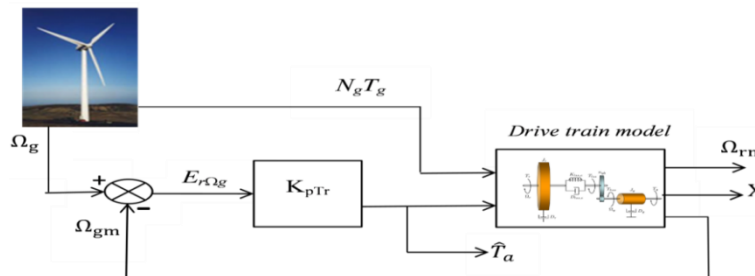


Fig. 4 Estimation scheme of the aerodynamic torque

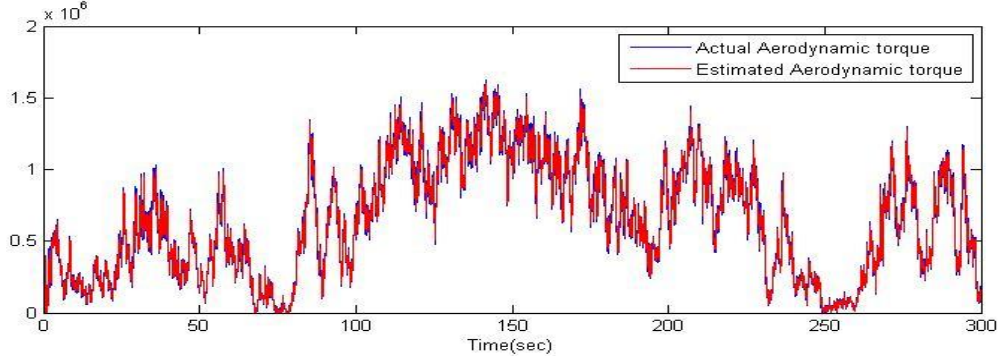


Fig. 5 Estimated and actual aerodynamic torque (Nm)

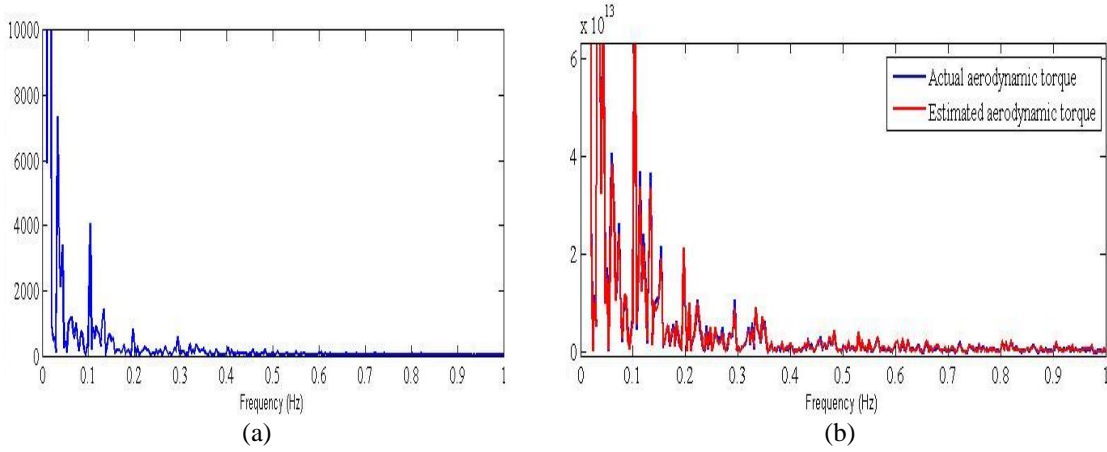


Fig. 6 (a) Power spectral of the turbulent wind, (b) Power spectral density of the estimated and the actual aerodynamic torque

Note that K_{pTr} is the proportional torque estimator gain; $E_{r\Omega_g}$ is the speed tracking error, T_g is the generator torque about the high speed shaft, N_g is the gearbox ratio, the term $N_g T_g$ is the generator torque about the low speed shaft; Ω_{gm} is the model generator speed about low speed shaft; Ω_g is the measured generator speed; X is the restoring force of the low speed shaft; Ω_{rm} is the model rotor speed; \hat{T}_a is the estimated aerodynamic torque.

Define the mean convergence error between actual aerodynamic torque T_a and estimated aerodynamic torque \hat{T}_a along N samples of data

$$error(\%) = \frac{100}{N} \sum_{i=1}^N \left| \frac{T_{a,i} - \hat{T}_{a,i}}{T_{a,i}} \right| \quad (6)$$

In the present case of simulation, we obtain a relative error of 1.8%. The torque estimation could then be considered sufficiently accurate.

3.2 Estimated aerodynamic torque filtering

In this section, a spectral analysis of is performed to identify the frequencies of the wind speed transmitted to the torque and those resulting from the mechanical vibration. The objective is to reconstruct the frequencies specific to the wind speed. Figs. 6(a) and 6(b) show the power spectral density of the wind profile and aerodynamic torque respectively.

One can notice that the frequencies contained in the wind and having a significant effect on the torque of the rotor resides in the low frequency range (<0.12 Hz). The peaks that occur beyond this area are the result of vibrations of the mechanical structure as a result of excitations caused by the wind. The estimated aerodynamic torque, which will be used for reconstitution of the wind speed, should therefore be filtered according to the previous remark. In the case of our system, we chose a low pass filter of 0.4 Hz bandwidth. Fig. 7 shows the filtered aerodynamic torque. Fig. 8 shows the power spectral density of filtered and the non-filtered torque.

From Fig. 8, one can notice that frequencies above 0.4 Hz have been attenuated and filtered.

4. Wind speed estimation using the integrator based observer

4.1 Wind speed estimation loop

In the literature, the methods proposed up to now tried to extract directly the wind speed from the numerical resolution of Eq. (1). The direct numerical solution of Eq. (1) is unfortunately not evident for small pitch angles because the function $C_q(V, \Omega_r, \beta)\lambda^{-3}$ is non injective as studied in Østergaard *et al.* (2007). Our method is based on an indirect and online technique avoiding the previously mentioned constraint. An integrator based observer is used with Eq. (1) to derive the suitable V^2 responsible of making estimated torque sufficiently close to the calculated aerodynamic torque given by Eq. (7) bellow. The wind speed estimation is then obtained by calculating the root square of the previously estimated square wind speed. Fig. 9 shows the proposed estimation scheme of the wind speed. The structure of the integrator term is $\frac{T_i}{s}$.

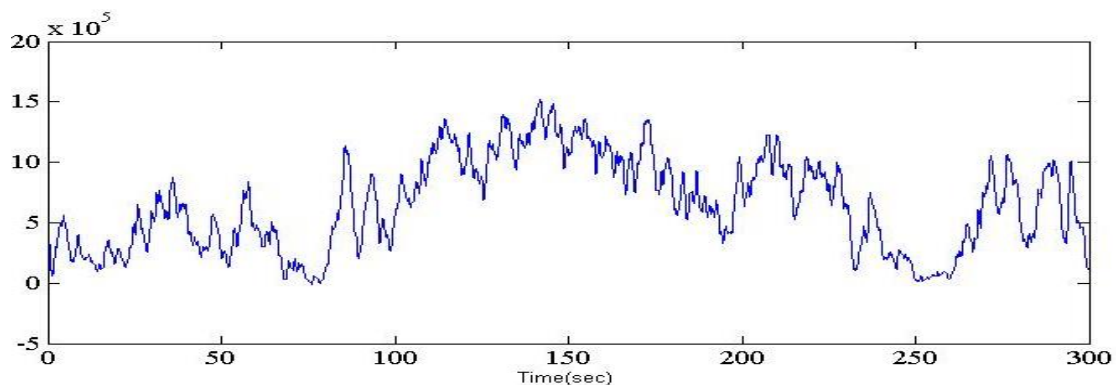


Fig. 7 Filtered aerodynamic torque (Nm)

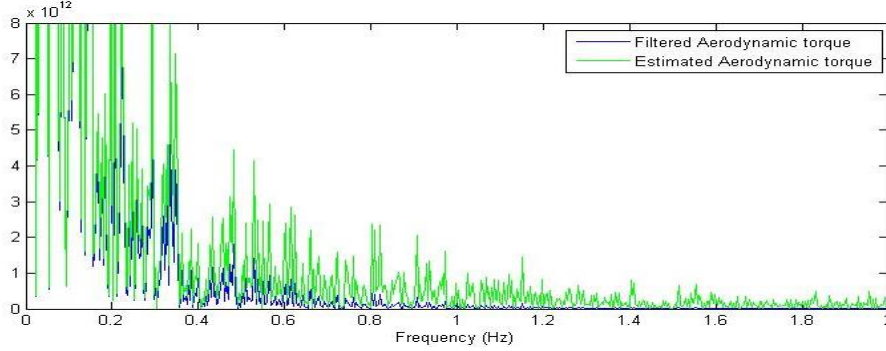


Fig. 8 Power spectral of the estimated and filtered aerodynamic torque

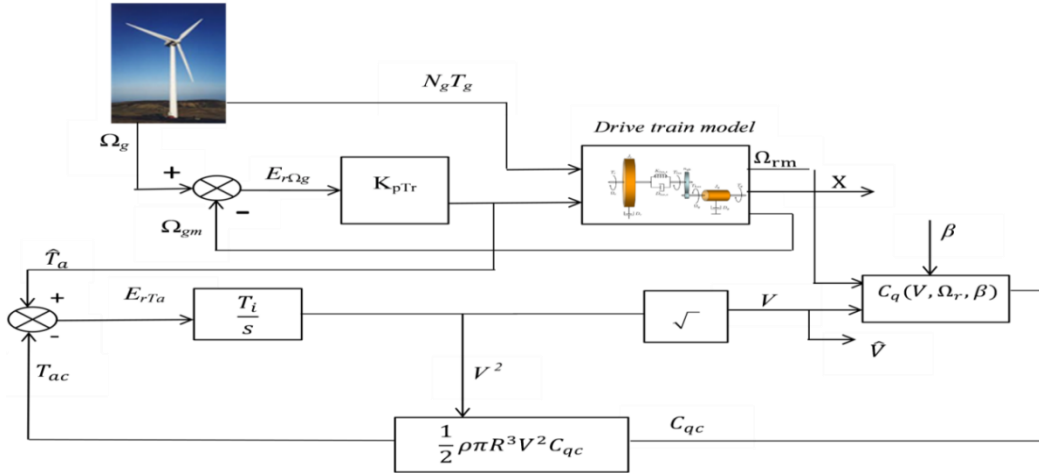


Fig. 9 Wind speed estimation scheme

Note that E_{rTa} is the torque loop error, $E_{r\Omega_g}$ is the torque estimator loop error, V is the wind speed, C_{qc} is the online calculated torque coefficient, Ω_g is the measured generator speed, Ω_{gm} is the model generator speed, \hat{T}_a is the estimated aerodynamic torque, T_{ac} is the online calculated aerodynamic torque, K_{pTr} is the proportional gain for the torque estimation loop and Ω_{rm} is the model rotor speed used to compute C_{qc} online. Let T_{ac} be the online calculated aerodynamic torque. It is given by

$$T_{ac} = \frac{1}{2} \rho \pi R^3 V^2 C_{qc}(V, \Omega_r, \beta) \quad (7)$$

Where $C_{qc}(V, \Omega_r, \beta)$ is the online calculated torque coefficient, which is bounded in the interval $[C_{qmin}; C_{qmax}]$; with $C_{qmin} = 0.001$ and $C_{qmax} = 0.16$. Recall that the coefficient torque C_q represents the amount of the extracted torque from the total available aerodynamic torque provided by the wind. For simplification, we will note C_{qc} instead of the term $C_{qc}(V, \Omega_r, \beta)$. The transfer function between the square of the wind speed and the estimated aerodynamic torque is

given by

$$V^2 = \frac{T_i}{s} (\hat{T}_a - T_{ac}) \tag{8}$$

By replacing Eq. (7) in Eq. (8) we obtain the observer transfer function

$$V^2 = \frac{1}{\gamma C_{qc} + \frac{s}{T_i}} \hat{T}_a \tag{9}$$

Where $\gamma = \frac{1}{2} \rho \pi R^3$ is a constant term depending on the radius of the blades R , and T_i is the observer integrator gain. Multiplying both sides of Eq. (9) by γC_{qc} we obtain

$$\gamma C_{qc} V^2 = \frac{\gamma C_{qc}}{\gamma C_{qc} + \frac{s}{T_i}} \hat{T}_a$$

This leads to the transfer function between the computed torque T_{ac} and the estimated one \hat{T}_a

$$T_{ac} = \frac{1}{1 + \frac{s}{\gamma C_{qc} T_i}} \hat{T}_a \tag{10}$$

$\tau_0 = \frac{1}{\gamma C_{qc} T_i}$ is the observer time constant and $f_0 = \frac{\gamma C_{qc}}{2\pi} T_i$ is the cut-off frequency of the observer. The frequency f_0 is fixed by the operator to reach a desired filtering capability of the observer, according to the spectral analysis in the section 3. In our case, f_0 is fixed to 0.3 Hz. T_i is then computed as $T_i = \frac{2\pi}{\gamma C_{qc}} f_0$. From the Eq. (10), the C_q value could influence the bandwidth of our observer. The worst case corresponds to C_{qmin} that gives the smallest bandwidth, Fig. 10. In order to keep sufficient distance from useful frequencies when filtering, C_{qmin} will be considered for the computation of the integrator term T_i . For C_q equal to C_{qmin} , $\frac{2\pi}{\gamma C_{qc}}$ will be equal to 0.0762. One can take the integrator gain T_i equal to $\frac{2\pi}{\gamma C_{qc}} f_0$.

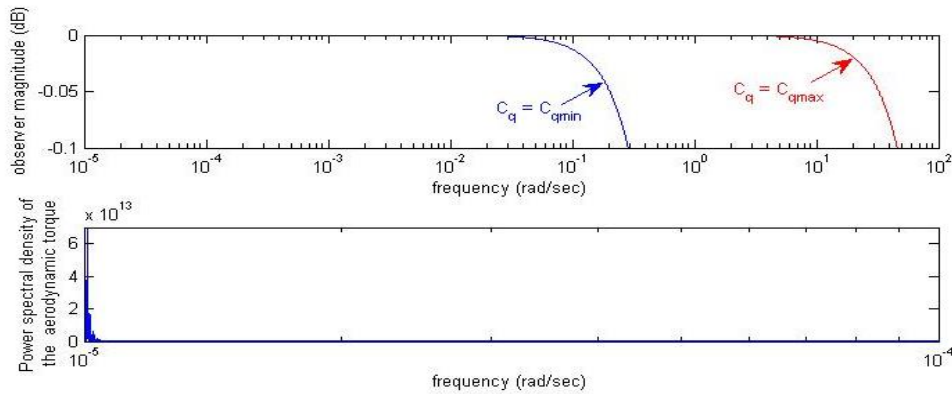


Fig. 10 Observer magnitude and power spectral density of the aerodynamic torque in the frequency domain

From Fig. 10, one can see that the useful frequencies of the aerodynamic torque reside in the frequency interval for which the observer gain is 0dB. The last means that the observer can reconstruct these frequencies in a perfect way.

4.2 Issues on the stability and convergence of the observer:

The transfer function between T_{ac} and \hat{T}_a is a stable first order system because τ_0 is positive. In fact, γ , f_0 and C_{qc} ($0 < C_{qmin} < C_{qc} < C_{qmax}$, during the normal operating region) are positive. From Eq. (10), for low frequency variations of the aerodynamic torque (when s tends to 0), T_{ac} converges to \hat{T}_a . Define the relative convergence error as

$$\varepsilon(\%) = 100 \frac{\hat{T}_a - T_{ac}}{\hat{T}_a} \quad (11)$$

Eq. (11) is equivalent to $\varepsilon(\%) = 100(1 - G_0(\omega))$.

Where $G_0(\omega) = \frac{1}{\sqrt{\tau_0^2 \omega^2 + 1}}$ is the gain of the observer. Every observable frequency ω (rad/s) should be less or equal than ω_0 , where $\omega_0 = 2\pi f_0 = 0.6\pi$ (we have taken $f_0 = 0.3$ Hz). After some manipulations, we obtain the final inequality

$$\varepsilon(\%) \leq 100 \left(1 - \frac{1}{\sqrt{\tau_0^2 \omega_0^2 + 1}}\right). \quad (12)$$

For $\omega_0 = 0.6\pi$, we obtain the relative error: $\varepsilon(\%) \leq 1\%$.

This result relies on the precision of (1.8%) between the estimated torque \hat{T}_a and the real torque T_a being defined in the section 3. Fig. 11 shows the actual (filtered) compared to the estimated wind speed. Fig. 12 shows the power spectral density of the two last results.

The accuracy of the estimation seems to be promising. Its effectiveness will be confirmed in section 5, in the control of the generator speed.

The comparison between the proposed algorithm and other existing algorithms could be done on the basis of three aspects: The implementation simplicity of the method, the need to restrictive conditions and the a priori needed information.

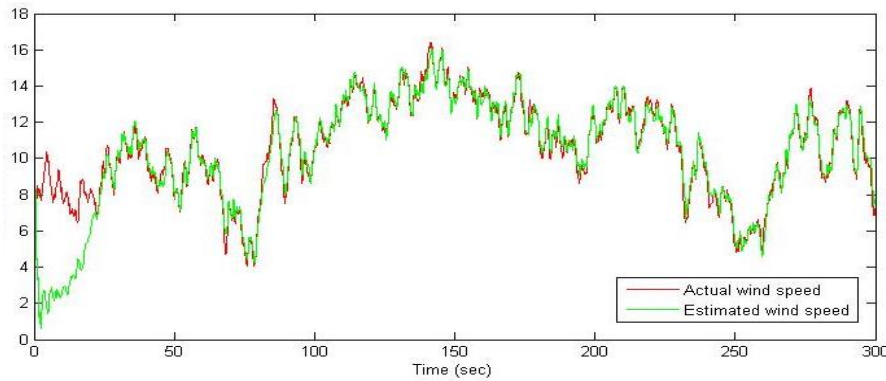


Fig. 11 Actual and estimated wind speed (m/s)

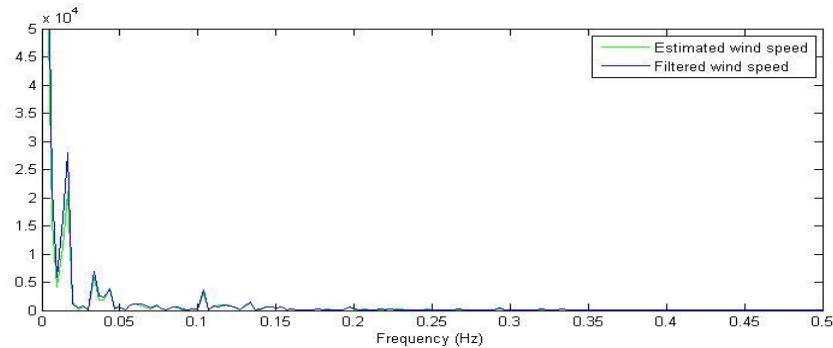


Fig. 12 Power spectral density of the actual (filtered) and estimated wind speed

Table 2 Comparative description between the presented method and existing industrial methods

The characteristics The methods	Restriction on the pitch angle	A priori knowledge of information	Implementation issues
The integrator based method (proposed in this paper)	Works with small pitch angles, even zero degree	No a priori knowledge is needed	Only an integrator term is needed to implement the method (could be implemented as a simple analog circuit)
Newton Raphson based methods	Could work with small pitch angles, but with additional conditions.	No a priori knowledge is needed	Accuracy and convergence time is related to the sampling step choice
Neural networks based methods	Works with small pitch angles, even zero degree	No a priori knowledge is needed	Memory and time consuming
Probabilistic distribution parameter estimation methods	Works with small pitch angles, even zero degree	An a priori knowledge of the distribution is needed (Kaimal, Von Karman, Weibull, ...)	Memory and time consuming due to distribution parameters (2 up to 4) estimation

According to the comparative table, we can conclude that, for the first criterion, the newton Raphson based method needs additional conditions on small pitch angles. The other methods works for small pitch angles unconditionally. Based on the second criterion, the probabilistic distribution based methods need an a priori knowledge on the nature of the distribution unlike the remaining methods. Concerning the implementation and configuration, the probabilistic based methods need estimation of many parameters (2 up to 4) of the a priori selected distribution law. The neural networks based algorithms are time and memory consuming. The newton Raphson method accuracy and convergence time are related to the used sampling time. For the proposed integrator based algorithm, only an integration parameter T_i is to be configured to refine the estimated useful wind speed.

5. Generator speed control using wind speed estimator

5.1 The control strategy

Let V_{Ω_N} be the wind speed leading to nominal rotational speed of the turbine and V_N the wind speed leading to nominal power of the turbine. The control strategy is focused on three control objectives. First, maximize energy at low wind speeds, when the wind speed is less than V_{Ω_N} , by keeping tip speed ratio at optimal value indicated by the constructor, (7 in our case). Second, keeping the generator speed at rated value when the wind speed is between V_{Ω_N} and V_N . Third, reduce loads and prevent turbine from destruction at high wind speeds by keeping power at its nominal value P_N for the wind speed exceeding V_N . Practically, these objectives are realized through a reference speed switching approach, based on the wind speed estimation and the following reference block of Fig. 13, illustrating the sensorless control structure used in this paper taken from Bianchi *et al.* (2011).

$$\Omega_{gref} = \begin{cases} \frac{\lambda_0 \tilde{V}}{R} & \text{if } \tilde{V} < V_{\Omega_N} \\ \Omega_N & \text{if } V_{\Omega_N} \leq \tilde{V} < V_N \\ \Omega_g : \frac{1}{2} \rho \pi R^2 C_p \left(\frac{R \Omega_g}{\tilde{V}} \right) \tilde{V}^3 = P_N & \text{if } \tilde{V} \geq V_N \end{cases} \quad (13)$$

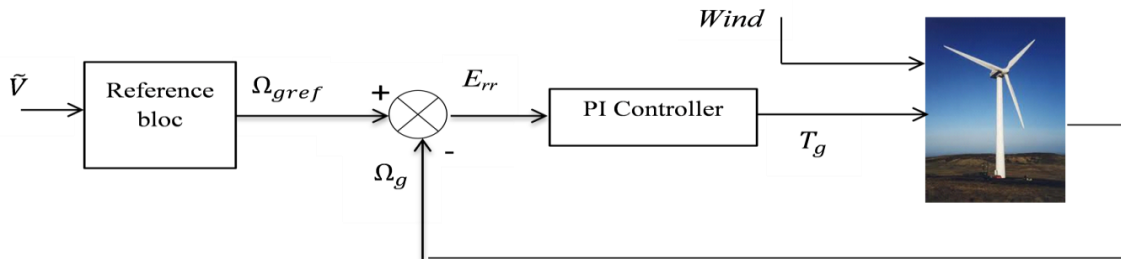


Fig. 13 The control system structure

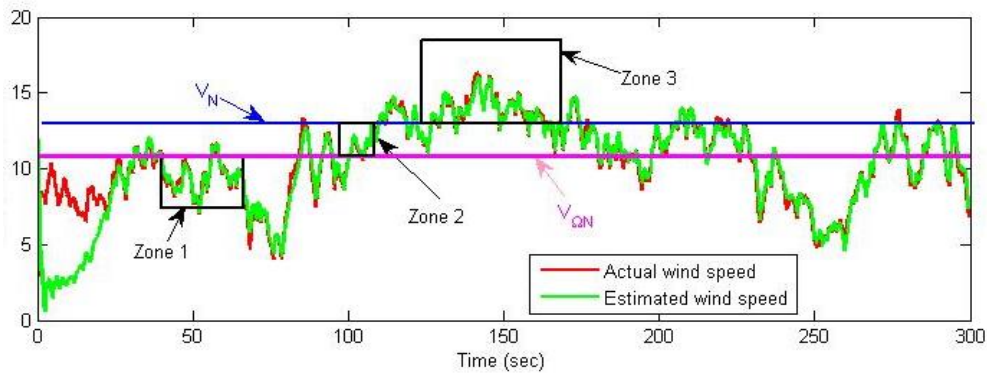


Fig. 14 The three zones of wind speed considered in simulation

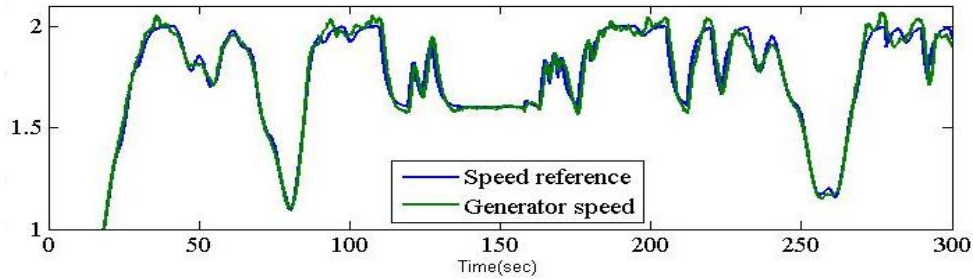


Fig. 15 Reference and generator speed (rad/s)

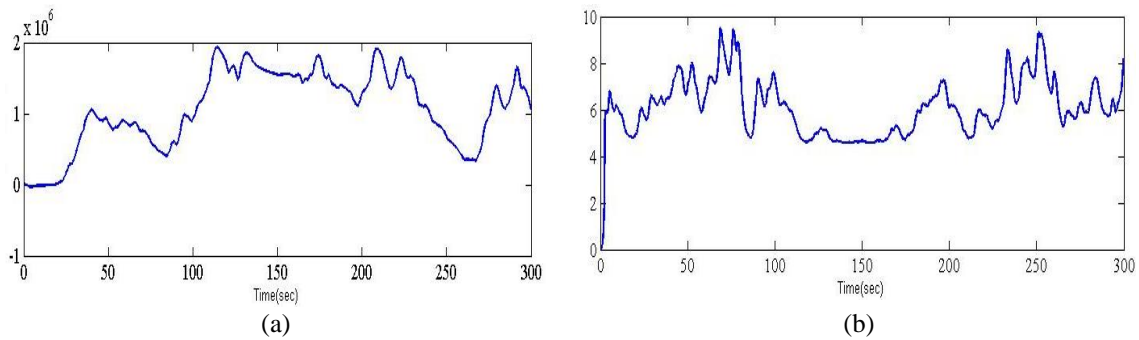


Fig. 16 (a) Rotor power and (b) tip speed ratio

The effectiveness of the wind speed estimation based control is illustrated in Figs. 14-19. Turbulent wind and all turbine degrees of freedom are activated. Thus, mechanical solicitations could introduce small additional variances and insignificant delays on the wind speed estimation. The surrounded zones represent some examples of previously mentioned control regions of the wind turbine. The three regions of operation for the wind turbine are illustrated in Fig. 14. The reference and the response of the generator speed in all the regions are shown in Fig. 15. The rotor power is illustrated in Fig. 16(a). In Fig. 16(b), the tip speed ratio is illustrated over the working region.

5.2 Wind speeds below the wind speed leading to rated generator speed ($V < V_{\Omega N}$)

Consider the zone corresponding to the time interval [30; 65] sec (zone1 in Fig. 14), in which the wind verifies $V < V_{\Omega N}$. The tip speed ratio corresponding to this zone is zoomed in Fig. 17. One can notice that while wind speed is under $V_{\Omega N}$, the algorithm tries to keep the mean of tip speed ratio around its optimum 7.

5.3 Wind speed between $V_{\Omega N}$ and V_N ($V_{\Omega N} \leq V < V_N$)

Consider the zone corresponding to the time interval [100; 110] sec (zone 2 in Fig. 14), in which $V_{\Omega N} \leq V < V_N$. The generator speed (about the low speed shaft) corresponding to the

previous zone is zoomed in Fig. 18. As can be expected, when wind speed is between V_{Ω_N} and V_N , the algorithm keeps the generator speed at its rated value Ω_N .

5.4 Wind speed above rated wind V_N ($V \geq V_N$)

Consider the zone corresponding to the time interval [125; 165] sec (zone 3 in Fig. 14), in which $V \geq V_N$. The rotor power corresponding to this zone is zoomed in Fig. 19. When wind speed exceeds the limit V_N , the algorithm tries to keep power at rated value to prevent damage of the structure.

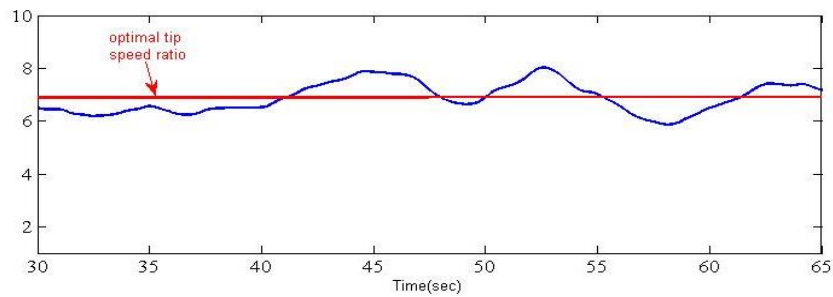


Fig. 17 Zoom on the tip speed ratio (λ) in the region [30; 65] sec

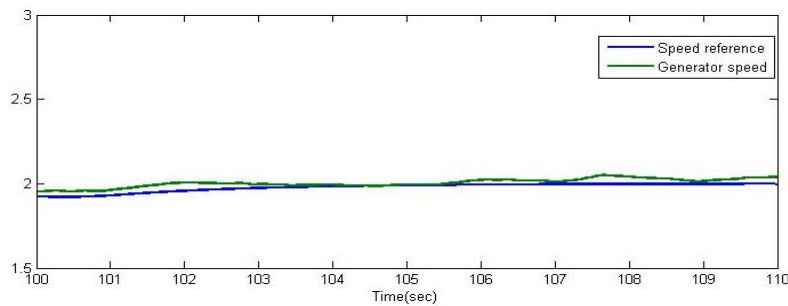


Fig. 18 Zoom on the generator speed in the region [100;110] sec

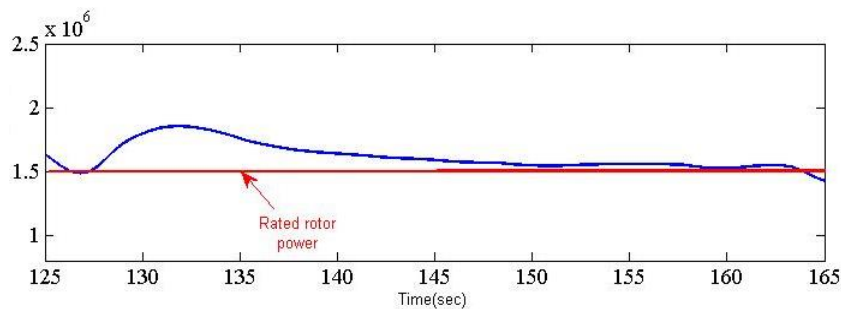


Fig. 19 Zoom on the power in the region [125;165] sec

6. Conclusions

In this work, the proposed approach for reconstructing the wind speed uses an integrator based observer. The method seems to be simple to configure and implemented in real time wind turbines. Compared to other existing methods, it doesn't need complex design tools and skills such as neural networks based methods. Also, the method works for small, even zero, pitch angles, without any restrictive condition on the monotonicity of the function $C_p(V, \beta, \Omega_r) * \lambda^{-3}$. The last advantage can be explained by that the method avoids direct numerical resolution of the Eq. (1).

The proposed method to estimate the wind speed has been tested and validated under turbulent wind. The considered wind profile follows the Kaimal distribution with 30% of disturbance. The obtained results showed good accuracy. The estimated wind speed was used in the control system loop in the three regions delimited by the $V_{\Omega N}$ and V_N wind speed. The approach could also be used in load alleviation and fault detection in anemometers which are relevant research axes.

References

- An, Y., and Pandey, M.D. (2005), "A comparison of methods of extreme wind speed estimation", *J. Wind Eng. Ind. Aerod.*, **93**(7), 535-545.
- Beltrán, J., Guerrero, J.J., Melero, J.J. and Llombart, A. (2014), "Detection of nacelle anemometer faults in a wind farm minimizing the uncertainty", *Wind Energ.*, **16**(6), 657- 669.
- Bhowmik, S. and Spee, R. (1998), "Wind speed estimation based variable speed wind power generation", *Proceedings of the 24th Annual Conference of the IEEE Industrial Electronics Society*, Aachen, August.
- Bianchi, F.D., Battista, H. and Mantz, R.J. (2011), *Wind Turbine Control Systems: Principles, Modelling and Gain Scheduling Design*, London, Springer.
- Bongers, P. (1994), *Modeling and identification of flexible wind turbines and a factorizational approach to robust control*, Ph.D. Dissertation, Delft University of Technology.
- Boukhezzar, B., Lupu, L., Siguerdidjane, H. and Hand, M. (2007), "Multivariable control strategy for variable speed, variable pitch wind turbines", *Renew. Energ.*, **32**(8), 1273-1287.
- Bourlis, D. and Bleijs, J.A.M. (2010), "A wind speed estimation method using adaptive kalman filtering for a variable speed stall regulated wind turbine", *Proceedings of the IEEE 11th International Conference on Probabilistic Methods Applied to Power Systems*, Singapore, June.
- Chauvin, J. and Petit, N. (2010), "Reconstruction of the fourier expansion of inputs of linear time-varying systems", *Automatica*, **46**(2), 354-361.
- Cutler, N.J., Outhred, H.R. and MacGill, I.F. (2012), "Using nacelle-based wind speed observations to improve power curve modeling for wind power forecasting", *Wind Energ.*, **15**(2), 245-258.
- Deepa S.N. and Sheela, K.G. (2014), "New criteria to fix number of hidden neurons in multilayer perceptron networks for wind speed prediction", *Wind Struct.*, **18**(6), 619-631.
- García, A., Torres, J.L., Prieto, E. and De Francisco, A. (1998), "Fitting wind speed distributions: a case study", *Sol. Energy*, **62**(2), 139-144.
- Hafidi, G. and Chauvin, J. (2012), "Wind speed estimation for wind turbine control", *Proceedings of the International Conference on Control Applications*, Dubrovnik, October.
- Hammerum, K., Brath, P. and Poulsen, N.K. (2007), "A fatigue approach to wind turbine control", *J. Phys. Conf. Ser.*, **75**(1).
- Hooft, E.L. Van Der, and Van Engelen, T.G. (2004), "Estimated wind speed feed forward control for wind turbine operation optimization", *Proceedings of the European Wind Energy Conference*, London, November.
- Hui, Y., Yang, Q. and Li, Z. (2014), "An alternative method for estimation of annual extreme wind speeds", *Wind Struct.*, **19**(2), 169-184.

- <http://wind.nrel.gov/designcodes/simulators/fast/>.
- <http://wind.nrel.gov/designcodes/preprocessors/turbsim/>.
- Jabbari, F. (1997), "Output feedback controllers for systems with structured uncertainty", *IEEE T. Automat. Contr.*, **42**(5), 715-719.
- Lee, J.W., Kim, J.K., Han, J.H. and Shin, H.K. (2013), "Active load control for wind turbine blades using trailing edge flap", *Wind Struct.*, **16**(3), 263-278.
- Jonkman, J.M. and Buhl, M.L. (2005), "Fast user's guide".
- Jonkman, J.M. and Buhl, M. L. (2007), "TurbSim user's guide".
- Justus, C.G., Hargraves, W.R., Mikhail, A. and Graber, D. (1978), "Methods for estimating wind speed frequency distributions", *J. Appl. Meteorol.*, **17**(3), 350-353.
- Kanev, S. and Van Engelen, T. (2010), "Wind turbine extreme gust control", *Wind Energ.*, **13**(1), 18-35.
- Khalil, W.H. (2007), "Modeling and performance of a wind turbine", *Anbar J. Eng. Sci.*, **1**(1), 116-130.
- Kodama, N., Matsuzaka, T. and Inomata, N. (2000), "Power variation control of a wind turbine generator using probabilistic optimal control, including feed-forward control from wind speed", *Wind Eng.*, **24**(1), 13-23.
- Kusiak, A. and Li, W. (2010), "Estimation of wind speed: a data-driven approach", *J. Wind Eng. Ind. Aerod.*, **98**(10-11), 559-567.
- Laks, J.H., Pao, L.Y. and Wright, A.D. (2009), "Control of wind turbines: past, present, and future", *Proceedings of the American Control Conference*, St. Louis, MO, June.
- Lombardo, F.T. (2012), "Improved extreme wind speed estimation for wind engineering applications", *J. Wind Eng. Ind. Aerod.*, **104-106**, 278-284.
- Mohandes, M., Rehman, S. and Rahman, S.M. (2011), "Estimation of wind speed profile using adaptive neuro-fuzzy inference system (anfis)", *Appl. Energ.*, **88**(11), 4024-4032.
- Novak, P., Ekelund, T., Jovik, I. and Schmidbauer, B. (1995), "Modeling and control of variable speed wind turbine drive-system dynamics", *IEEE Control Syst.*, **15**(4), 28 – 38.
- Ohtsubo, K. and Kajiwara, H. (2004), "Lpv technique for rotational speed control of wind turbines using measured wind speed", *Proceedings of the Oceans*, Kobe, November.
- Østergaard, K.Z., Brath, P. and Stoustrup, J. (2007), "Estimation of effective wind speed", *J. Phys. Conf. Ser.*, **75**(1).
- Pao, L.Y. and Johnson, K.E. (2009), "A tutorial on the dynamics and control of wind turbines and wind farms", *Proceedings of the American Control Conference*, St. Louis, MO, June.
- Perrin, O., Rootzén, H. and Taesler, R. (2006), "A discussion of statistical methods used to estimate extreme wind speeds", *Theor. Appl. Climatol.*, **85**(3-4), 203-215.
- Sedghi, M., Hannani, S.K. and Boroushaki, M. (2015), "Estimation of weibull parameters for wind energy application in Iran", *Wind Struct.*, **21**(2), 203-221.
- Seguro, J.V. and Lambert, T.W. (2000), "Modern estimation of the parameters of the weibull wind speed distribution for wind energy analysis", *J. Wind Eng. Ind. Aerod.*, **85**(1), 75-84.
- Sloth, C., Esbensen, T., and Stoustrup, J. (2011), "Robust and fault-tolerant linear parameter-varying control of wind turbines", *Mechatronics*, **21**(4), 645-659.
- Spencer, M.D., Stol, K.A., Unsworth, C.P., Cater, J.E. and Norris, S.E. (2013), "Model predictive control of a wind turbine using short-term wind field predictions", *Wind Energ.*, **16**(3), 417-434.
- Wright, A.D. (2004), "Modern control design for flexible wind turbines".
- Wright, A.D. and Balas, M.J. (2003), "Design of state-space-based control algorithms for wind turbine speed regulation", *J. Sol. Energy Eng.*, **125**(4), 386.
- Wright, A.D., Fingersh, L.J. and Stol, K. (2007), "Designing and testing controls to mitigate tower dynamic loads in the controls advance research turbine".
- Wu, S., Wang, Y. and Cheng, S. (2013), "Extreme learning machine based wind speed estimation and sensorless control for wind turbine power generation system", *Neurocomputing*, **102**, 163-175.